Hindawi
Advances in Civil Engineering
Volume 2022, Article ID 4958566, 12 pages
https://doi.org/10.1155/2022/4958566

Research Article

Shield Cutting Pile-Group Implementation Effects on the Superstructure

Chi Zhang,[1] Shiju Ma ,[2] Yuancheng Guo,[1] Mingyu Li,[1] and Kui Fu[3]

[1]*School of Civil Engineering, Zhengzhou University, Zhengzhou, China*
[2]*School of Civil Engineering, Zhengzhou Institute of Technology, Zhengzhou, China*
[3]*China Railway 18th Bureau Group First Engineering Co. LTD, Baoding, Hebei, China*

Correspondence should be addressed to Shiju Ma; mashiju2010@126.com

Received 21 July 2022; Revised 18 August 2022; Accepted 24 August 2022; Published 27 September 2022

Academic Editor: S. Mahdi S. Kolbadi

Copyright © 2022 Chi Zhang et al. This is an open access article distributed under the Creative Commons Attribution License, which permits unrestricted use, distribution, and reproduction in any medium, provided the original work is properly cited.

The shield tunneling method is widely used in urban subway construction. However, as the layer stress state changes during shield tunnel construction, layer displacement and surface deformation occur accordingly. This study tries to investigate the settlement and deformation of the masonry structure in shield cutting the composite foundation of group piles in a shield tunnel project at Zhengzhou Metro Line 5. To understand the distribution characteristics and changing rules of building settlement during the process of shield cutting group piles composite foundation passing through the masonry structure, a thorough analysis of the ground surface settlement and building settlement, including on-site measured, was conducted. The results show that piles go down through a composite foundation during shield cutting. The cumulative maximum settlement and maximum differential settlement of the masonry structure were concentrated at the intersection of the tunnel axis and the building. The longitudinal distribution of the cumulative settlement of the south and north wall of the masonry structure changes continuously with the change of the position of the shield excavation surface. That behavior may cause the building to be tilted and deformed and cause the structure to undergo rigid rotation and twisting deformation. Based on the composite pile foundation project of the Shield Tunnel Cutting Group in a specific section of Zhengzhou Metro Line 5, this paper analyzes the surface settlement and foundation settlement data of the building caused by the construction of the shield. It obtains the changes of the surface settlement and the settlement of the foundation of the building. No other changes have been made to the existing cracks in the external walls of the building. At the same time, because of the low angle between the longitudinal axis of the masonry structure and the tunnel axis (22°) and the positive effect of the ring beam and column of the structure in the building, it is clear that the construction of this project has little effect on the upper building, thus showing improved control.

1. Introduction

With the rapid development of the urban subway system, an increasing number of tunnels are being built in China. However, tunneling deforms the surrounding soil and adjacent structures, such as buildings, existing tunnels, and buried pipelines. Therefore, minimizing the interference of the tunnel construction process on nearby structures has been the focus of engineers and researchers in the field of geotechnical engineering. Usually, this kind of displacement and deformation can be completed in a short time, and this kind of rapid deformation is very destructive to the superstructure. Many scholars have investigated the damage to the upper structures caused by shield tunnel construction. In terms of theory, Burland and Wroth [1] and Burland et al. [2] proposed a classification standard of damage level of masonry structure based on the concept of ultimate tensile strain. They applied it to the influence of tunnel excavation on upper buildings. Boscardin and Cording [3] and Boone [4] treat buildings as elastic beams and then propose a

method to define the failure level by angular distortion and horizontal strain. Burland [5] and Clarke and Laefer [6] proposed a method to define the failure level by the horizontal strain and deflection ratio. In terms of field measurement, Dimmock and Mair [7] compared and analyzed the bending deformation and strain of the building caused by shield construction and the deformation and strain of the surface based on the measured data and concluded that the stiffness of the upper building has a corrective effect on the settlement caused by the tunnel. Camós et al. [8] observed buildings' settlement, deformation, and damage through shield tunnel construction. They found that the vertical and horizontal displacement of the ground is often reduced because of the existence of buildings.

Underground pile foundations are dense in cities with crowded buildings. If the distance between the pile foundation and the shield is too close, tunneling may cause uneven settlement, deformation of the structure, and cracks in the building [9]. Zhang et al. [10] studied the impact of the shield tunnel crossing underneath a river on bridge piles under the working conditions without rainfalls and concluded that the scheme of erecting up temporary inverted arches and grouting under-the-bridge piles for water plugging was feasible and that the grouting effect was critical to the construction of under-the-bridge undercutting piles.

With the development of the urban underground space, the cases of shield tunnel digging under or adjacent to the existing pile foundations of buildings are increasing. Tunnel construction inevitably redistributes the initial soil stress and causes surface settlement, tilting, curvature change, horizontal displacement, and discontinuous deformation that may affect the adjacent pile foundations, resulting in potential safety hazards for the structure to bring constructions. Breth and Chambosse [11] and Frischmann et al. [12] studied and analyzed the ground subsidence caused by tunnel excavation. Forth and Thorley [13] believed that the main reason for the reduction of pile side friction resistance caused by shield construction was the vertical displacement of the stratum towards the tunnel. Miliziano et al. [14] used two-dimensional numerical simulation methods to study the impact of tunnel construction on adjacent buildings in terms of numerical analysis. Giardina et al. [15], Giardina et al. [16], and Giardina et al. [17] established two-dimensional and three-dimensional finite element models to evaluate the damage degree of adjacent masonry structures caused by surface settlement caused by tunnel construction under different working conditions. Burd et al. [18] established a three-dimensional finite element model of tunnel-soil-building integration considering the weight and stiffness of the building. The results of their study showed that the interaction between the soil and the structure would reduce the damage degree to the building. Underground structures, especially tunnels, are very common, especially in urban areas [19]. Nevertheless, studies that investigate the influence of the underground structures on the dwelling structures are very sporadic. Furthermore, to the best of our knowledge, there is no study that analyzes the settlement and deformation of the masonry structure in shield cutting the composite foundation of group piles in a shield tunnel.

Furthermore, we propose cost-effective methods for real-time tracking and control of building settlement. Therefore, the main goal of this study is to better understand the interaction between underground and surface masonry structures, i.e., the investment effect of a tunnel in masonry construction meetings. Also, the paper suggests some cost-effective monitoring and mitigation measures. The rest of the paper is organized as follows: Section 2 provides a brief description of the stud case, Section 3 describes the most common methods for monitoring settlements, Section 4 details the monitoring and analysis of construction settlements for the case this study took into consideration, Section 5 describes surface settlements and the most critical areas, and Section 6 discusses the consequences of settlements on building stability. Finally, the main conclusions and recommendations from this study are presented in Section 7.

2. Engineering Situation

Shield cutting soil-cement group piles composite foundation in Zhengzhou Metro Line 5 passes through the building project. The mileage of the left line of the pile cutting construction section is DK13 + 662.558~DK13 + 711.322 (685 rings ~ 715 rings, the length is about 48.764 m), and the tunnel forms an angle of 22° with the plane of the existing house, as shown in Figure 1.

There are about 224 agitating piles intruded by the shield. The length of the shield cutting pile is about 2.6~3.7 m. The outer diameter of the segment is 6.2 m, the inner diameter is 5.5 m, the wall thickness is 0.35 m, and the width of the lining ring is 1.5 m. The segment material is C50 concrete, and the segment assembly method adopts staggered seam assembly. The building is a 7-story masonry structure with a semi-basement, and the foundation form is a strip foundation. The foundation is treated with a cement-soil pile composite foundation. The pile length is 11.5 m, the pile diameter is 0.5 m, and the spacing between the piles is 0.95 m. The exterior of the building is shown in Figure 2.

3. Settlement Control Measures

As shown in Figure 3, two "gaps" need to be mainly controlled during shield construction, namely clearance between shield and shield tail and clearance between cutter and shield, to reduce the adverse impact on the masonry structure and foundation during the construction process of the shield machine cutting piles.

This paper uses three "Clay shock" grouting methods, synchronized grouting, and secondary reinforcement grouting to control the surface settlement and building settlement.

3.1. Clay Shock Method. Eight radial grouting holes with a diameter of 12 mm are arranged along the circumference of the shield body at the middle shield position in the shield machine (Figure 4). Grouting is carried out synchronously to the outside of the shield machine shell, which is the gap between the shield body and the outer soil body. Grouting can form a reliable sealing water-blocking clay grouting layer

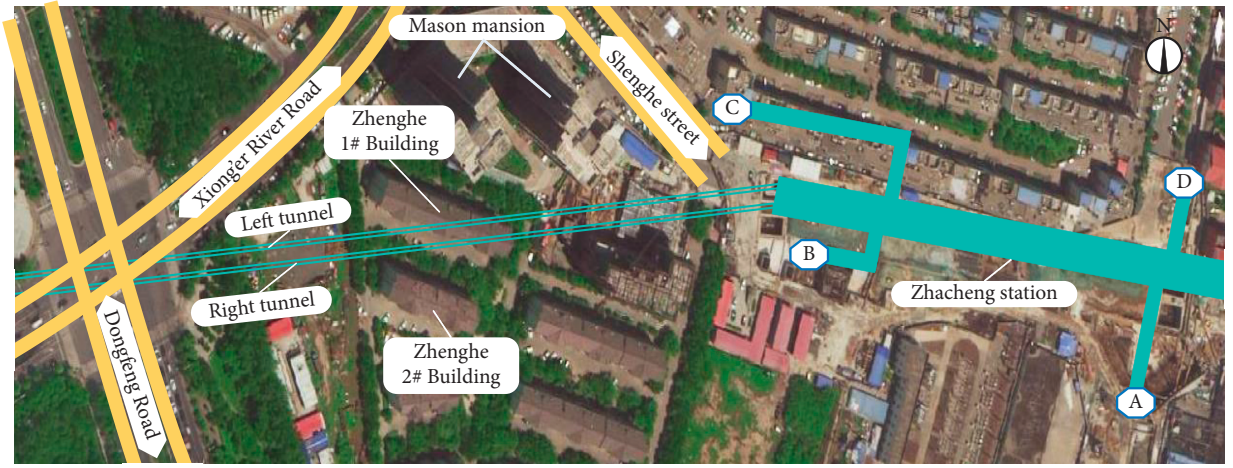

Figure 1: Plan view of shield tunnel cut pile passing through masonry structure.

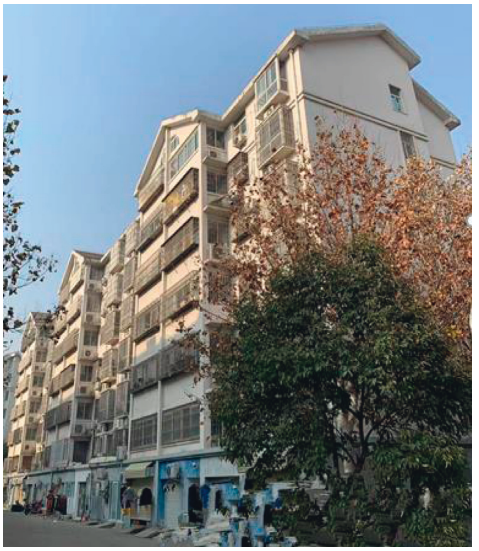

Figure 2: The appearance of a masonry structure.

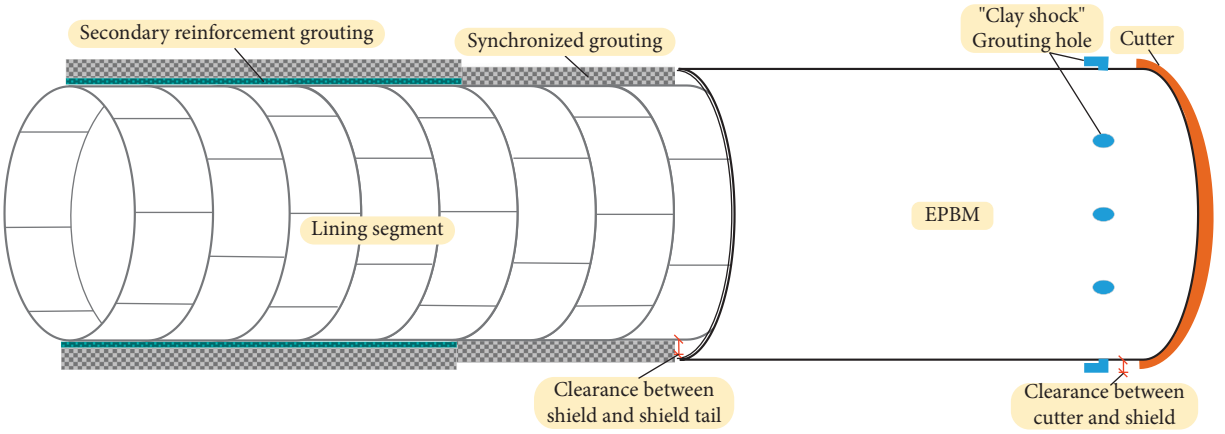

Figure 3: Schematic diagram of formation subsidence control principle.

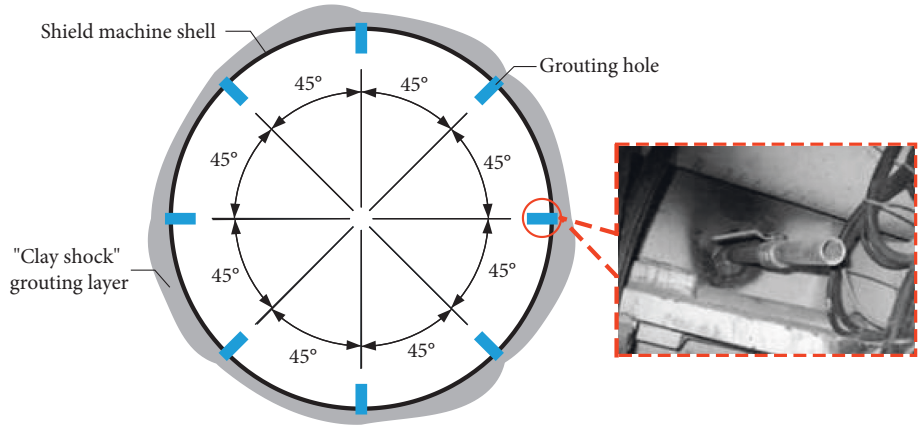

Figure 4: The layout of grouting holes in the shield machine shell.

around the shield machine, filling the gap between the shield and the stratum and effectively controlling the amount of soil subsidence during excavation. The injection process of "Clay shock" grouting is controlled as follows: the "Clay shock" grouting starts at the first ten rings of passing the building. Before the shield machine starts to advance, inject A liquid first and then B liquid. Prevent pipe blockage caused by the mixing of water glass with clay slurry.

The grouting pressure is 0.2~0.4 MPa. "Clay shock" grouting is synchronized with propulsion, and the grouting speed should be adjusted according to the propulsion speed. Inject 1.26 m^3 of mixed solution (140% of the theoretical value) into each ring. The ratio of "Clay shock" grouting is shown in Table 1.

3.2. Synchronized Grouting. When the lining structure is separated from the shield tail, fill the building gap between the shield machine shell and the lining structure on time and prevent the composite foundation from sinking rapidly in a short period. The synchronous grouting measures at the shield machine's shield tail are taken. The theoretical building gap caused by advancing the single-ring segment is $1.5 \times \pi \times (6.442–6.22)/4 = 3.57$ (m^3), and the initial setting time of the slurry was about 4 hours. The actual grouting volume is 150%~200% of the theoretical building space of each ring segment, i.e., the synchronous grouting volume for each advancing ring is 8 m^3, and the pressure at the pumping outlet is generally controlled at 0.3~0.4 MPa. The slurry pressure should also be adjusted and controlled according to ground and building settlement. The slurry ratio is shown in Table 2.

3.3. Secondary Reinforcement Grouting. To reduce the late settlement of the soil after the shield machine and reduce the waterproof pressure of the tunnel, secondary reinforcement grouting is carried out after the segment is separated from the 6^{th} to 8^{th} rings of the shield tail. Moreover, a double slurry composed of cement slurry and water glass is selected to quickly fill the gap between the grouting layer remaining in the synchronous grouting and form a certain strength. The ratio of the double slurry is shown in Table 3.

The grouting sequence is injected according to the method of "first dome, then two waists, and two waists are symmetrical." After filling one ring, the grouting of the next ring is carried out. The standard of filling is that no water flows out after the lifting hole of the ring is opened. The secondary grouting pressure is controlled at ⊁0.5 Mpa.

4. Settlement Measurement

According to the requirements of "Technical Specifications for Urban Rail Transit Engineering Monitoring" [20, 21] and "Urban Rail Transit Engineering Measurement Specifications" [22, 23], combined with the actual project site overview and building characteristics, three surface subsidence monitoring sections, namely DB1, DB2, and DB3, were set up. The measuring points of the building foundation settlement are arranged clockwise along the corner of the building, numbered JG1~JG19. There are 19 measuring points in total. See Figure 5–7 for the relative positional relationship between the building and the tunnel and the layout method of monitoring points.

5. Surface Settlements

The surface subsidence process caused by shield construction is divided into five stages: stage I is before the shield reaches the monitoring section. In stage II, the shield passes through the monitoring section. Stage III is the shield tail prolapse monitoring section. In stage IV, shield cut pile group composite foundation passed. Stage V is the subsequent subsidence stage. The DB1 monitoring section is located at the cross-section of the 685 rings of the left-line tunnel. The shield cutter head of the left-line tunnel cuts into the composite foundation and starts to cut piles. It can be seen from Figure 8 that, in stage I, each monitoring point of the DB1 monitoring section showed slight uplift, and the maximum uplift value appeared on the right line tunnel outline. In stage II (III), the measuring point DB1-1 on the center of the left tunnel and the measuring point DB1-2 on the outline of the left tunnel appeared to sink because of shield excavation and pile cutting. In contrast, the centerline of the right tunnel and the corresponding measuring points

Table 1: The ratio of "Clay shock" grouting.

Material name	Proportion	Dosage (m^3)	Volume weight (kg/m^3)	Coagulation time (s)	Viscosity (dPa·s)
Liquid A: special bentonite liquid Liquid B: water glass mixture	20 : 1	"Clay shock" powder 400 kg, 40 Baumé degree, water glass dosage 70 kg, water 846 kg	2600	4.5 s start to cement, 20 s initial setting.	300~500

Table 2: Synchronous grouting slurry ratio table.

Cement (kg)	Fly ash (kg)	Bentonite (kg)	Sand (kg)	Water (kg)
170	400	800	750	450

Table 3: Secondary grouting slurry ratio table.

Material name	Material parameters	Proportion	Coagulation time (s)	28 days strength (Mpa)
Cement Water glass	P.O 42.5 Baumé degree: 30~35, modulus: 2.8~3.1	Water : Water glass : Cement slurry = 3 : 1:1 (volume ratio)	30	2.6

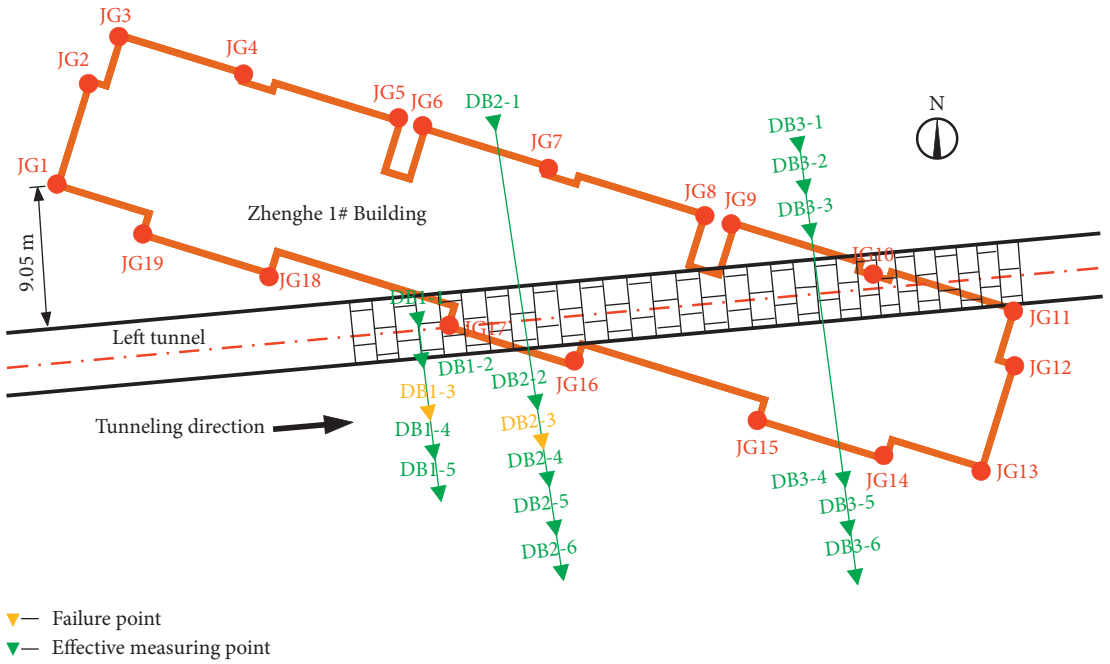

Figure 5: The relative position between building and tunnel and the plan of monitoring instruments.

DB1-4 and DB1-5 on the outline of the tunnel on the right line is uplifted. It is because of synchronous grouting and the "Clay shock" method when the shield cuts piles. The extruded soil effect caused the pile body that was not damaged by the shield to bulge slightly upwards, which triggered the ground surface to bulge. In stage IV, all measuring points of this monitoring section subside. The settlement law and settlement amount of the measuring points on the centerline and outline of the left tunnel are generally consistent, and the settlement value is greater than that of the measuring points on the right tunnel. In stage *V*, the monitoring points of the DB1 monitoring section first subsided and then gradually rose. Finally, the subsidence was stable until the shield tail protruded for 15 days. The maximum occurred at the centerline of the left tunnel, and the subsidence value was −9.0 mm.

As shown in Figure 9, before the shield reaches the DB2 monitoring section, i.e., stage I, each measuring point of this monitoring section is slightly uplifted. Nevertheless, the maximum uplift point appears at the two monitoring points, DB2-1 and DB2-2, closest to the building, which is different from the maximum uplift position of the DB1 monitoring section. In stage II (III), affected by the existing cement-soil group pile composite

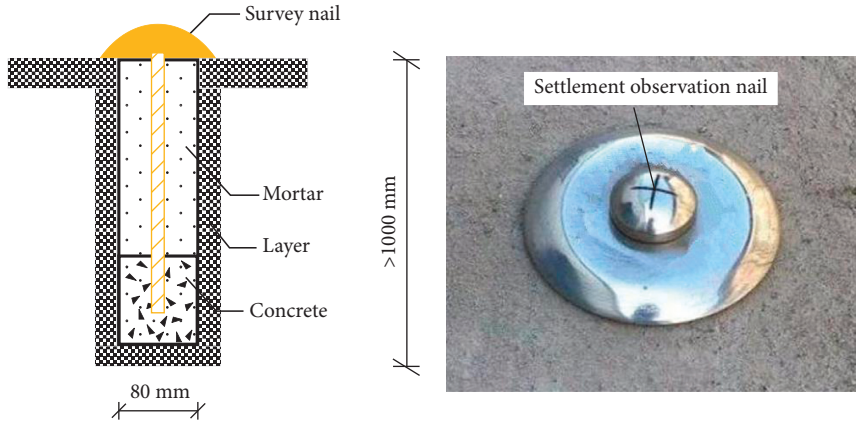

Figure 6: Buried method and physical map of surface subsidence measuring points.

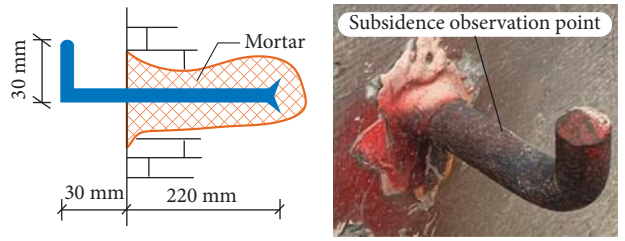

Figure 7: Layout method and physical map of building foundation settlement monitoring points.

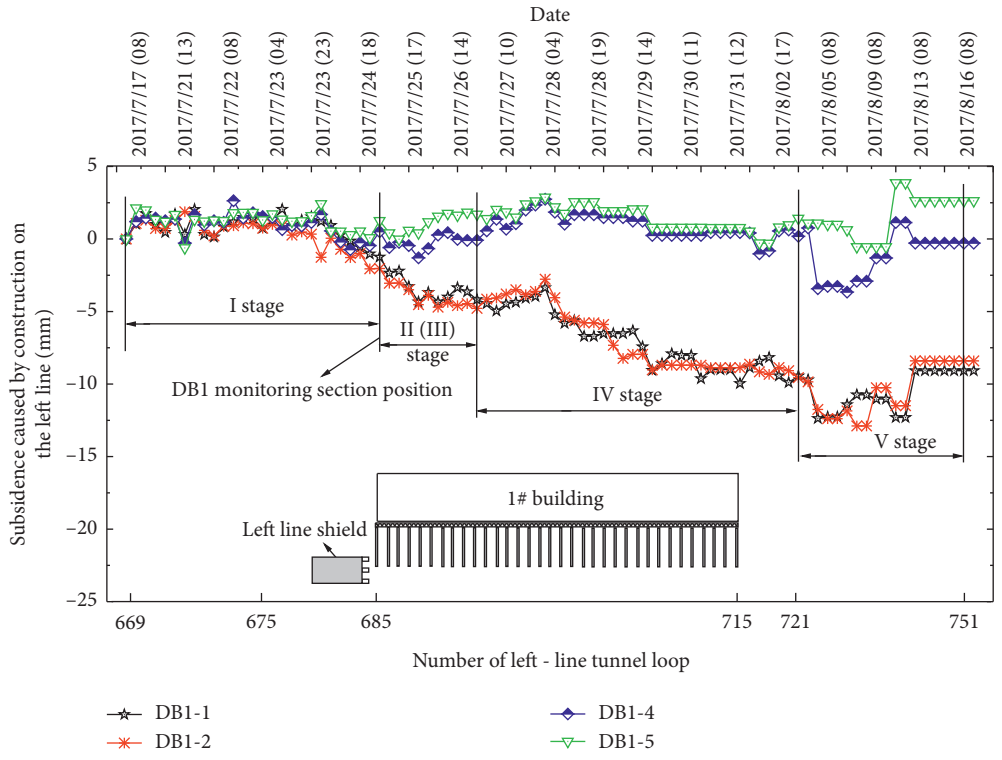

Figure 8: Monitoring time-history curve of surface subsidence of section 1.

foundation, the changes of each measuring point of the DB2 monitoring section at this stage are small, except for the DB2-2 measuring point that is closer to the centerline of the left line of the tunnel, which sinks slightly. In addition, all other measuring points have uplifted, and the uplift value is not large. In stage IV, the shield tail was separated from the monitoring section and continued to cut piles. All monitoring points were affected by the

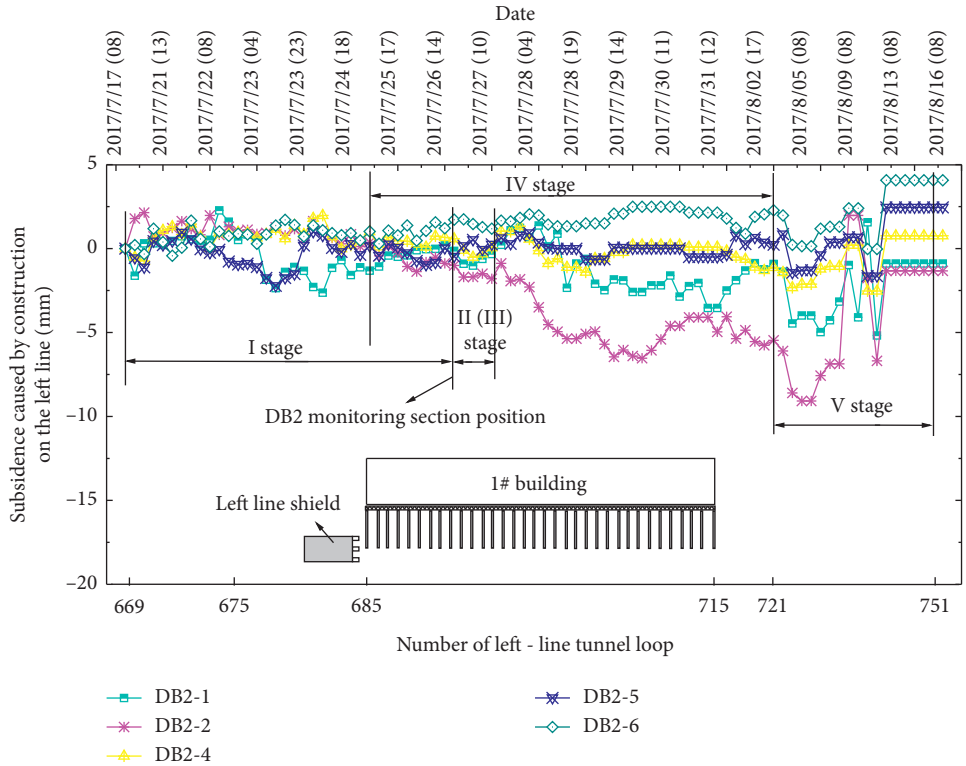

Figure 9: Monitoring time-history curve of surface subsidence of section 2.

construction disturbance of shield cutting and pile cutting, and they sank. The maximum settlement occurs near the intersection point of the left-line tunnel cutting into the building. The settlement value is −6.5 mm. In the stage, each measuring point of the surface settlement presents a "*W*" shape, closely related to the secondary grouting amount of the shield and the grouting amount of "Clay shock" grouting. The position of the maximum settlement value at this stage is the DB2-2 measuring point, the settlement value is −9.0 mm, and the settlement value of this measuring point after stabilization is −0.89 mm.

As shown in Figure 10, the monitoring points DB3-1, DB3-2, and DB3-3 subsided in stage I. The maximum subsidence occurred at the monitoring point DB3-1, with a value of −3.5 mm. The monitoring points of DB3-4, DB3-5, and DB3-6 are slightly uplifted, the maximum uplift value is +2.4 mm, and the maximum uplift point is the DB3-4 measurement point. It is caused by the uneven settlement of the building caused by the construction of the left shield line cutting piles. In stage II, as the shield cutting piles are excavated through the DB3 monitoring section, the monitoring points closer to the left line of the tunnel have the largest settlement.

In contrast, the measuring points arranged on the south side of the right line of the tunnel are slightly uplifted. In stage III, apart from the gradual sinking of the DB3-3 measuring point, the DB3-1 and DB3-2 measuring points were affected by the simultaneous grouting and secondary grouting and presented an uplift. In contrast, the DB3-4 and DB3-5 on the south side of the building were uplifted. DB3-6 monitoring point side changes gently, indicating that grouting effectively controls the surface settlement and building inclination caused by tunnel pile cutting. Stage IV includes stages I, II, and III, and hence, no analysis is done.

6. Effects on Building

6.1. Building Response. As shown in Figures 11 and 12, the settlement time-history curves of the north and the south wall of the building show that the settlement value of each settlement measurement point of the south wall is slightly larger than that of the north wall. However, the variation range of each settlement measurement point of the south wall is smaller than that of the north wall. Before the left line of the shield reaches the building, each measuring point on the north wall presents a bulge, and the maximum bulge value is +5.59 mm, which is located at the JG5 measuring point. The measuring point of the south wall is slightly sunk, and the maximum settlement is −2.21 mm. It is located at the JG1 measuring point (i.e., the southwest corner of Building 1). The left-line cutter head of the shield cuts into the pile group composite foundation until the shield tail escapes away from the composite foundation. Cutting the pile group composite foundation on the left line, measuring the building's settlement above the left line of the tunnel outline, and measuring the south wall's JG17 and JG16 points are all parts of the process. The most dangerous locations are JG10 and JG11 measuring points on the North Wall, whereas JG17 and JG16 measuring points on the

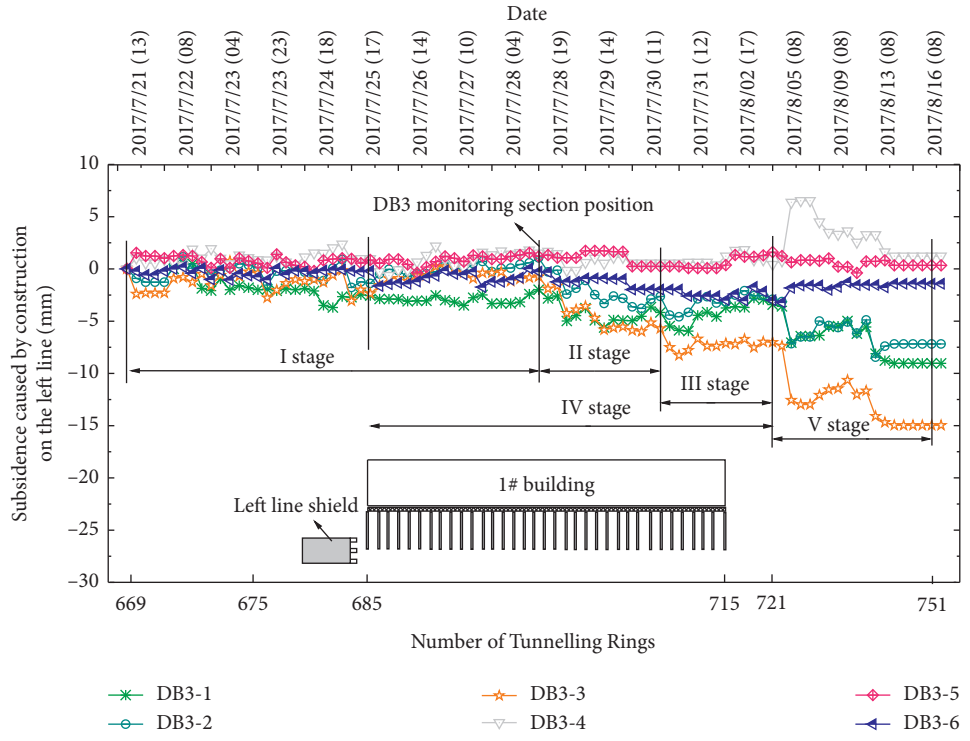

Figure 10: Monitoring time-history curve of surface subsidence of section 3.

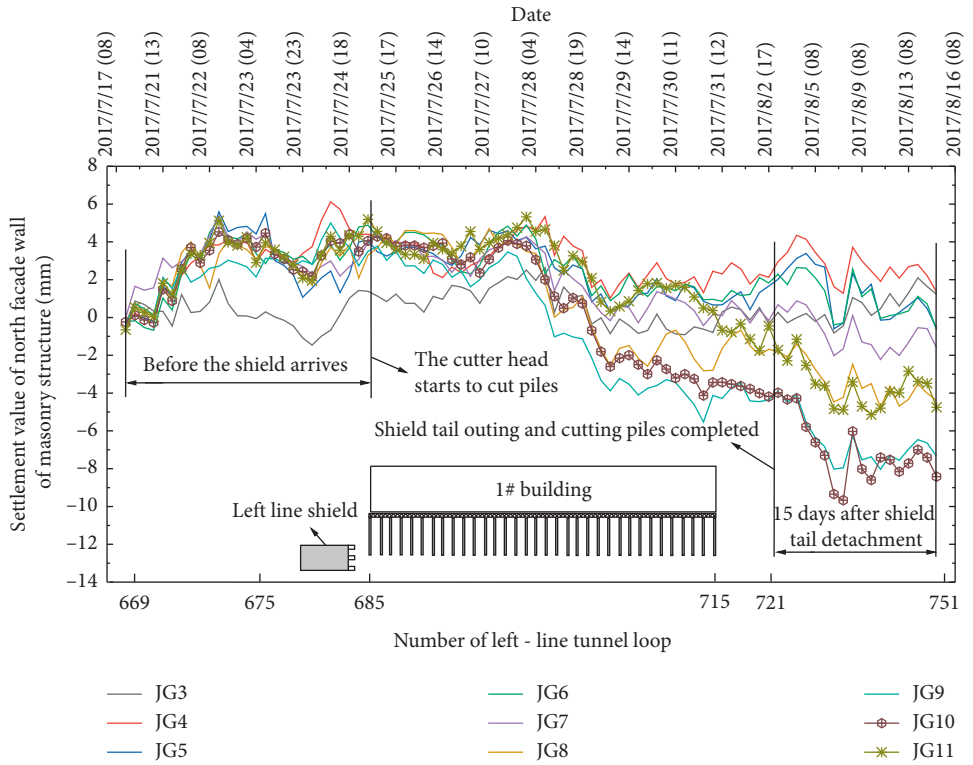

Figure 11: Settlement time-history curve of north facade wall of the building.

South Wall have settlement variation ranges of +3.49 mm ~ −5.79 mm, +4.3 mm ~ −2.53 mm, respectively. 15 days after the shield tail of the left line was protruded, the settlement values of the measuring points JG17 and JG16 on the south wall were -8.66 mm and -10.98 mm, respectively, and the settlement values of the measuring points JG10 and JG11 on the north wall were −9.63 mm and −7.76 mm, respectively.

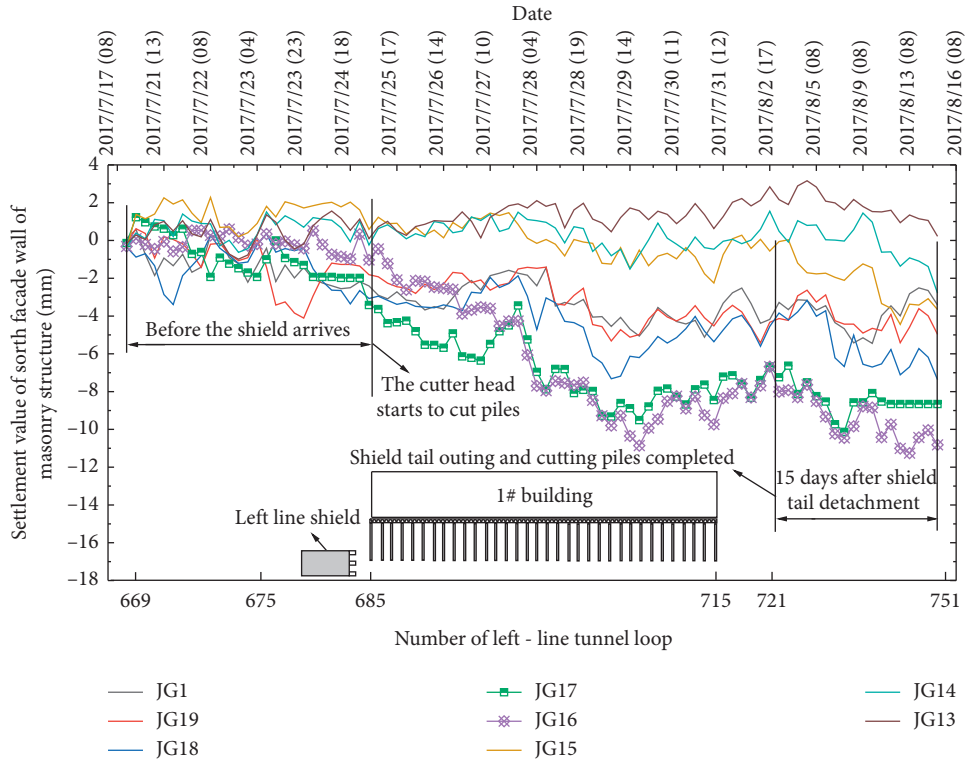

Figure 12: Settlement time-history curve of south facade wall of the building.

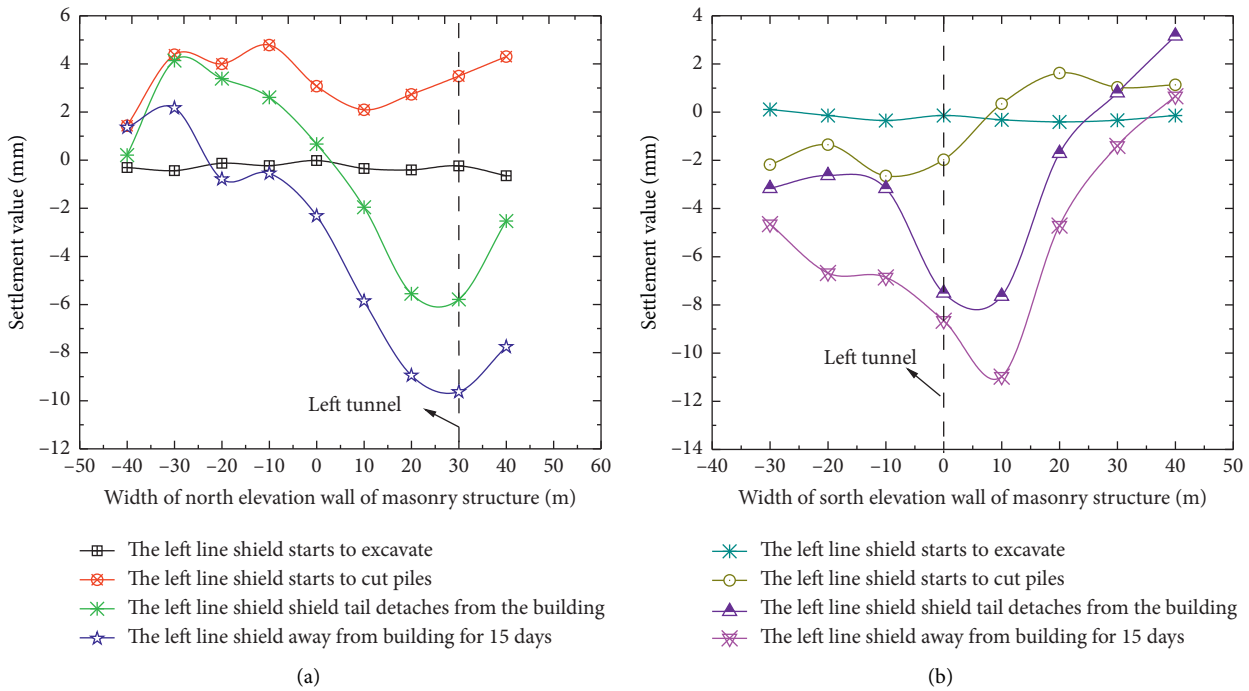

Figure 13: The settlement curve: (a) north facade and (b) south facade wall of the building at the critical moment.

Figure 13 shows the characteristic curves of the settlement distribution at the critical moment of the north and south walls of the building. It can be seen from the figures that the influence range of the shield tunnel construction on the ground settlement and the building settlement is different. The former is the tunnel axis 1.5 D. The latter involves the entire building. When the shield construction causes the settlement of one side of the building, the rigid building will rotate, resulting in the overall tilt of the building. Comparing Figures 13 and 14(a), it can be seen that

(a) (b)

Figure 14: Cracks (a) between the wall and outside apron slope and (b) on the basement floor.

Figure 15: Cracks on the first floor of the masonry structure.

the excavation construction of shield cutting piles causes the building as a whole to incline to the south, because the maximum settlement value position occurs at the oblique intersection of the tunnel and the building space.

6.2. Building Damage Assessment. As shown in Figures 14 and 15, when the shield construction of the left line is far away from 1# building for 15 days, the crack survey of the building structure shall be carried out above the building. The technical construction measures for sediment settlement are effective.

A crack with a length of 1.2 m and a width of 1.0~1.5 cm appeared between the wall at the northwest corner of the masonry structure and the scattered concrete water. A uniform crack with a length of 1.6 m and a width of 0.6 cm appeared on the ground in the northeast corner of the basement. A vertical crack with a length of 0.8 m and a width of 0.15 cm appeared on the first-floor wall at the southwest corner of the masonry structure.

According to "Code for Design of Building Foundation" (GB50007) [21] and "Standard for Appraisal of Dangerous Buildings" (JG J125) [22] and Limiting Tensile Strain Method (Limiting Tensile Strain Method), structural damage was analyzed. For measuring points JG1-1 and JG1-3, the differential settlement is 4.6 mm, and the slope is $i = 0.2‰$. For measuring points JG1-11 and JG1-13, the differential settlement is 5.8 mm, and the slope is $i = 0.3‰$. For measuring points JG1 -16 and JG1-07, the differential settlement is 10.7 mm, and the slope is $i = 0.6‰$. The ultimate tensile strain of the masonry structure is 7%.

7. Conclusions

Based on the theory of ultimate tensile strain to control building deformation, crack investigation and building damage assessment are carried out after construction, which confirms the effectiveness of building settlement control technology and innovative measures proposed in this research. The maximum value of surface settlement caused by shield construction occurs near the tunnel's axis on the left line. Because of the existence of the existing buildings, the surface settlement is relatively gentle for some time after shield construction. With the completion of the shield cutting group pile composite foundation, the surface settlement is larger than the building settlement. In the shield-cutting pile group composite foundation, the cumulative maximum settlement and the maximum differential settlement of masonry structure are concentrated at the intersection of the tunnel axis and building. The masonry structure is subjected to complex forces. In addition to the inclined deformation caused by differential settlement, the structure also has rigid rotation and distortion.

When the shield cutting piles construction, it is more beneficial to control the settlement and deformation of the house by stabilizing the pressure of the soil bin, increasing the amount of synchronous grouting and increasing the rotational speed of the cutter head. After the shield tail is separated from the house, the construction parameters should not be greatly adjusted, the cutter head pressure and Jack thrust should be appropriately increased, and the cutter head torque, cutter head speed, synchronous grouting amount, and tunneling speed should be kept unchanged, which is more conducive to controlling the settlement of the house. The settlement of ground surface and buildings can be effectively controlled using the "Clay shock" method and synchronous grouting during shield cutting piles construction. Secondary reinforcement grouting is carried out after the segment is separated from the 6th to 8th rings of the shield tail. The grouting sequence of each ring is injected according to the method of "first arch, then two waists, and two waists are symmetrical," which can effectively control the settlement after construction.

The subsequent settlement after construction is mainly affected by secondary grouting and the amount of "Clay shock" grouting. The maximum settlement monitoring point is the DB3-3 monitoring point, and the maximum settlement value after stabilization is −14.97 mm. The strength characteristics of the north wall and the south wall of the building are different. From the settlement curve formed after the shield was removed from the building for 15 days, it can be seen that the south wall approximately exhibits the force characteristic of the cantilever beam, while the north wall approximately exhibits the mechanical characteristics of the beam support. The whole process of building the shield tunnel causes the uneven settlement of the building, tilting of the building, and twisting deformation of the building.

Data Availability

The data used to support the findings of this study are available from the corresponding author upon request.

Conflicts of Interest

The authors declare no conflicts of interest.

Acknowledgments

The remarkable assistance from China Railway 18th Engineering Bureau Group First Engineering Co., Ltd, is highly appreciated.

References

[1] J. B. Burland and C. Wroth, "Settlement of buildings and associated damage," in *Proceedings of the Settlement of Structures*, pp. 611–654, London, England, January 1975.

[2] J. B. Burland, B. B. Broms, and V. F. De Mello, "Behaviour of foundations and structures," in *Proceedings of the 9th International Conference on Soil Mechanics and Foundation Engineering*, pp. 495–546, Tokyo, Japan, 1978.

[3] M. D. Boscardin and E. J. Cording, "Building response to excavation-induced settlement," *Journal of Geotechnical Engineering*, vol. 115, pp. 1–21, 1989.

[4] S. J. Boone, "Ground-movement-related building damage," *Journal of geotechnical engineering*, vol. 122, no. 11, pp. 886–896, 1996.

[5] J. Burland, "Assessment of risk of damage to buildings due to tunnelling and excavatioins," in *Proceedings of the 1st Internaional Conference on Earthquake Geotechnical Engineering*, Tokyo, Japan, 1995.

[6] J. A. Clarke and D. F. Laefer, "Evaluation of risk assessment procedures for buildings adjacent to tunnelling works," *Tunnelling and Underground Space Technology*, vol. 40, pp. 333–342, 2014.

[7] P. S. Dimmock and R. J. Mair, "Effect of building stiffness on tunnelling-induced ground movement," *Tunnelling and Underground Space Technology*, vol. 23, no. 4, pp. 438–450, 2008.

[8] C. Camós, C. Molins, and O. Arnau, "Case study of damage on masonry buildings produced by tunneling induced settlements," *International Journal of Architectural Heritage*, vol. 8, no. 4, pp. 602–625, 2014.

[9] P. Li, Y. Lu, J. Lai, H. Liu, and Ke Wang, "A comparative study of protective schemes for shield tunneling adjacent to pile groups," *Advances in Civil Engineering*, vol. 2020, Article ID 6964314, 16 pages, 2020.

[10] X. G. Zhang, L. Ju, and F. Li, "Analysis on and countermeasures for mining tunneling of line 14 of beijing Metro crossing underneath existing bridge piles," *J. Tunnel Construction*, vol. 35, no. 7, pp. 692–697, 2015.

[11] H. Breth and G. Chambosse, "Settlement behavior of buildings above subway tunnels in Frankfurt clay," in *Proceedings of the Conference on Settlement of Structures*, pp. 329–336, London, England, 1974.

[12] W. W. Frischmann, J. E. Hellings, G. Gittoes, and C. Snowden, "Protection of the mansion house against damage caused by ground movements due to the docklands light railway extension," *Proceedings of the Institution of Civil Engineers - Geotechnical Engineering*, vol. 107, no. 2, pp. 65–76, 1994.

[13] R. Forth and C. B. Thorley, "Hong Kong Island line-predictions and performance," in *Proceedings of the Geotechnical Aspects of Underground Construction in Soft Ground*, pp. 677–682, Roterdam, Netherlands Europe, 1996.

[14] S. Miliziano, F. Soccodato, and A. Burghignoli, "Evaluation of damage in masonry buildings due to tunnelling in clayey soils," in *Proceedings of the Geotechnical Aspects of Underground Construction in Soft Ground*, pp. 335–340, 2002.

[15] G. Giardina, M. A. N. Hendriks, and J. G. Rots, "Numerical analysis of tunnelling effects on masonry buildings: the influence of tunnel location on damage assessment," *Advanced Materials Research*, vol. 133-134, pp. 289–294, 2010.

[16] G. Giardina, M. A. N. Hendriks, and J. G. Rots, "Damage functions for the vulnerability assessment of masonry buildings subjected to tunneling," *Journal of Structural Engineering*, vol. 141, no. 9, Article ID 04014212, 2015.

[17] G. Giardina, M. A. N. Hendriks, and J. G. Rots, "Sensitivity study on tunnelling induced damage to a masonry façade," *Engineering Structures*, vol. 89, pp. 111–129, 2015.

[18] H. J. Burd, G. T. Houlsby, C. E. Augarde, and G. Liu, "Proceedings of the Institution of Civil Engineers," *Geotechnical Engineering*, vol. 143, no. 1, pp. 17–29, 2000.

[19] M. Ghorbani, M. Sharifzadeh, S. Yasrobi, and M. Daiyan, "Geotechnical, structural and geodetic measurements for conventional tunnelling hazards in urban areas – the case of

Niayesh road tunnel project," *Tunnelling and Underground Space Technology*, vol. 31, pp. 1–8, 2012.

[20] L. Wang, S. Xu, J. Qiu et al., "Automatic monitoring system in underground engineering construction: review and prospect," *Advances in Civil Engineering*, vol. 2020, Article ID 3697253, 16 pages, 2020.

[21] J. Yan, X. Liu, X. Bai et al., "Research on surface subsidence of long-span underground tunnel," *Advances in Civil Engineering*, vol. 2021, Article ID 6643892, 13 pages, 2021.

[22] Z. Chen, C. Qin, J. Tang, and Y. Zhou, "Experiment research of dynamic stray current interference on buried gas pipeline from urban rail transit," *Journal of Natural Gas Science and Engineering*, vol. 15, pp. 76–81, 2013.

[23] Y. Xu, P. Deng, R. Wang et al., "Influences of GPS point coordinate selection on Metro intersection area control network," *IOP Conference Series: Materials Science and Engineering*, vol. 780, Article ID 062050, 2020.